



CAS 2022

ANNUAL MEETING

June 24 - 26

Halifax, NS

2022 CAS Annual Meeting

Occupational Health and Risk Education

(Abstracts and Case Report/Series)

The Effect of Ventilation on Airborne Pathogen Exposure and Interaction with Passive Source Control: A Computational Fluid Dynamics Simulation and Tracer Gas Study

Authors:

Sjaus, Ana^{1,2}; d'Entremont, Matthew I.³; Ryan, Ben F.³; Munro, Allana^{1,2}; McKeen, Dolores⁴; Hung, Orlando¹

¹ *Dalhousie University, Faculty of Medicine, Department of Anesthesiology, Pain Management and Perioperative Medicine, Halifax, Nova Scotia, Canada*

² *IWK Health Center, Halifax, Nova Scotia, Canada*

³ *Nova Scotia Product Design and Development Centre, Dalhousie University, Halifax, Nova Scotia, Canada*

⁴ *Memorial University of Newfoundland, Faculty of Medicine, St. John's, Newfoundland, Canada*

Introduction:

SARS-Cov-19 has created an urgency to re-explore methods to control airborne transmission of respiratory pathogens. In addition to improved ventilation and masking, a variety of containment enclosures have been suggested as source control (SC) in cases when masking of diseased patient is not feasible.^{1,2,3} Studies of passive enclosures showed conflicting results, however most failed to account for the effect of ambient airflow.

We examined the effects on pathogen exposure and interactions across levels of air exchanges per hour (ACH), balance (positive vs negative) and the presence or absence of passive enclosure SC. Pathogen contamination was simulated by measured nitrous oxide, a tracer gas commonly used to mimic the spread of infectious aerosols.⁴ Computational fluid dynamics (CFD) simulation and physical experiments of N₂O distribution were conducted in three ventilation environments. Relative pathogen exposure was estimated and comparisons made with and without passive containment (a flexible enclosure partially open to the environment) around the source.

Methods:

Ethics approval was waived by the institutional committee. Recreation of operating room environments and boundary conditions was performed using detailed measurements and specifications¹⁹⁷ (Dessault Systemés, MA, USA). Three spaces were modelled: positive flow with 27 ACH (H), positive flow with 12 ACH (M) and a low negative flow room with 9 ACH (LN). Simulating contamination by patients' breathing, 50% N₂O/O₂ was released at 4 L/min. N₂O iso-surfaces were used to generate plumes which visually depicted areas where specific gas concentrations could be sampled. Streamlines showed recirculation patterns.

Tracer was sampled at 45 s intervals using gas analyzer (MiranSapphire SL, ThermoFisher Scientific, MA, USA) in two health care worker positions, with and without SC (12 conditions). To minimize the environmental impact, N₂O release from Aisys CS2 Carestation (GE Healthcare, USA) was stopped when measurement reached 100 ppm (0.01%).

Correction for decaying baseline and normalization by volume of released N₂O were performed prior to analysis. Sampling point measurements were paired by periods and compared within strata using Friedman test. Correlogram, differencing, moving average and trend functions were used in time series analysis. Relative

effect of factors was examined by fitting CART regression model to log transformed measurements (Minitab v.19, and STATA v.16).⁵

Results:

Simulation showed distinct areas of pooling of N₂O in all rooms. [Fig 1a] Streamline density and boundary volumes were reduced by SC to varying extents. Predicted relative retention of N₂O within SC enclosure was H=86.50%, M=61.90%, LN=91.90%.

The highest peak, mean and cumulative measurements were in room with lowest ACH. Ventilation had significant main effect and interaction with sampling positions (Chi(2)=68.8516, p=0.0000) and SC (Chi(2)=66.2778, p=0.0000). Autocorrelation, non-stationarity and skewness precluded classical modelling. Each of the time series was divided into contamination and decay segments and linear trends fitted. Peaks were delayed by SC in all environments. [Fig.1b] Slope and intercept decreased in M and trend was quadratic rather than linear in LN without SC. During decay, trend coefficients in M and LN were decreased by SC. A 13 node CART model best explained the data (R² 0.51, MSE 0.158), showing ventilation as the relatively the most important (90.0%) predictor of measurements (SC, 30.3%).

Discussion:

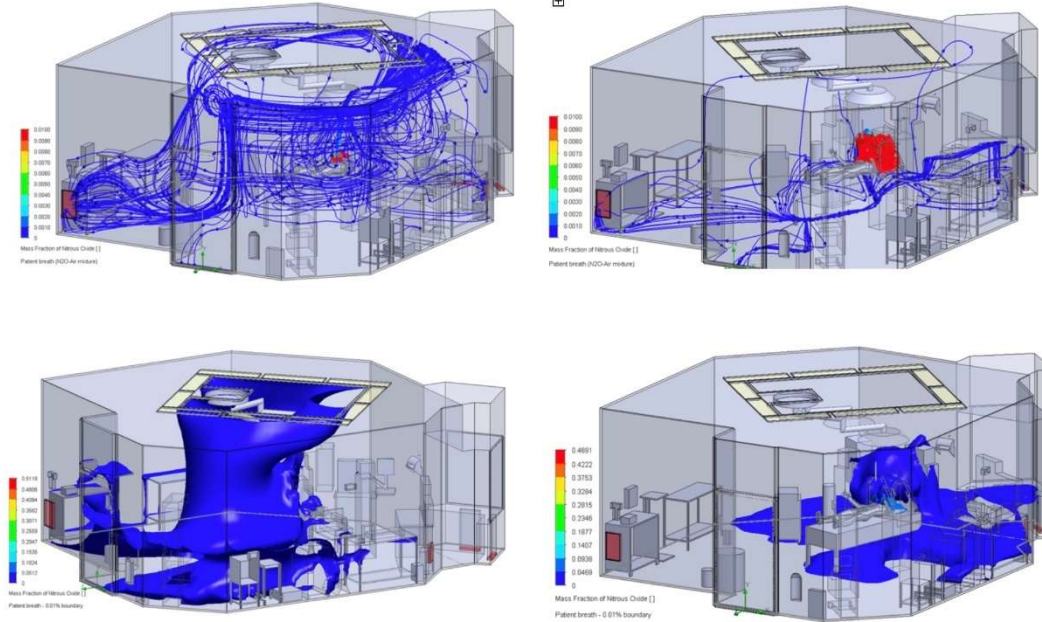
Ventilation had the largest effect on exposure (inverse relationship), with passive SC showing 30% of the relative effect. CFD allowed visualization of contaminant distribution: zones of high exposure away from the source in moderate-high ACH operating rooms and pooling in breathing zone of the negative flow room. Ventilation was a modifier for SC effect which was greatest for low ventilation, negative flow room. Passive enclosure acted as a concentrator and a reservoir, lowering the rate or release of the contaminant. These findings show the importance of combining CFD with physical experiments in studies of occupational exposure in engineered environments.

References:

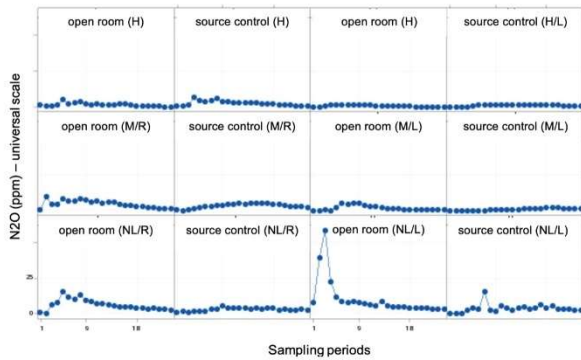
1. The Journal of Emergency Medicine 61, 695-704 (2021).
2. Journal of Anesthesia 382 (2021).
3. Indoor Air 31, 1639-1644 (2021).
4. Indoor Air 27, (6) (2017).
5. Neural Comput & Applic 31, 9023–9039 (2019).

Figure 1.

a. CFD in environment M showing flow trajectories in open (left upper) and source controlled (upper right) simulations. Iso-surface at 0.01% (100 ppm) boundary in open room (left lower) and with source control (lower right). Below, time series plots of all experiments (left), and key values (right).



Time series plots of measured N2O in H, M and NL environments (R and L sampling site)



Ventilation environment	average N2O in open room (ppm)	cumulative N2O (ppm)	change in cumulative N2O attributed to source control	average pairwise SC effect size for each paired sample (ppm)
H 26.9 ACH "positive" flow N=96	median (IQR) 1.32 (0.51, 1.55)	sampling site 37.57 R 18.778 L	(%) sampling site + 72.98 R + 30.10 L	median (IQR) 0.83 (0.59, 0.97)
M 11.9 ACH "positive" flow N=96	2.7 (1.59, 4.9)	113.35 R 43.36 L	- 27.62 R - 48.45 L	0.53 (-3.23, 1.14)
NL 8.9 ACH "negative" flow N=96	5.98 (3.73, 9.6)	145.61 R 242.88 L	-46.06 R - 65.79 L	-0.92 (-3.85, -0.33)

b. Trend graph for H, M and NL, with and without source control showing increases in lag and changes in contamination and decay trends. *note scale adjustments

